On the Dynamical Prediction of Large-Scale Condensation by Numerical Methods

JOSEPH SMAGORINSKY

U. S. Weather Bureau, Washington 25, D. C.

Abstract—The paper discusses properties of the hydrothermodynamic frameworks thus far employed, the approximations regarding the microphysics of precipitation, the quality of results of numerical integrations for different models, further work in the construction of more sophisticated dynamical models, and investigations of the relation of large-scale liquid water content and of water vapor, and the implications for the dynamical prediction of cloud formation and dissipation.

A brief survey of the state of the art—Attempts to make dynamical precipitation forecasts by numerical means began over 5 years ago. The first efforts were merely to employ the vertical motions calculated during the course of baroclinic numerical forecasts [*Smagorinsky* and *Collins*, 1955; *Miyakoda*, 1956; and *Smebye*, 1958]. The hydrodynamics were quasi-geostrophic, the baroclinic structure was described by information at three levels, and the potential vorticity was linearized when it appeared undifferentiated. Furthermore, the released latent heat was not permitted to add energy to the system.

It was assumed that precipitation occurred upon attaining saturation, but it was already realized that the space-averaged relative humidity need not be 100% for condensation or precipitation to occur. The possibility of supersaturation, supercooling, evaporation from falling drops, or inadequate nucleation was ignored. The results were reasonably encouraging, but further work suggested that departures from observation were to a large extent a result of errors in the large-scale hydrothermodynamics. The most obvious defect was the neglect of released latent heat, which is a destabilizing effect [*Smagorinsky*, 1956; *Aubert*, 1957]. This alone can amplify the large-scale upward vertical motions by as much as an order of magnitude giving maxima as large as 50 cm/sec. The degree of destabilization increases with decreasing scale and decreasing static stability.

It was also possible to remove the mathematical limitations of quasi-linearization and to add the barotropic effects of large-scale mountains. Since these models now possessed energy sources and moisture sinks it was desirable to provide a pseudo-boundary layer which would allow for surface friction and evaporation depending on land or sea. The quasi-geostrophic model equations have been recast to be governed instead by the balance (or quasi-non-divergent) condition [*Smagorinsky* and collaborators, 1959]. The results are often better, especially in the movement of the systems, but also suffer because of new limitations introduced. The relatively smaller characteristic scale of moisture distributions present special difficulties and somewhat special numerical techniques have been devised to reduce truncation error.

Although very distinct progress has been made, the remaining hydrodynamic degeneracies leave 24-hour precipitation forecasts with much to be desired. It is quite obvious that the geostrophic approximation as well as the balance condition are really valid for the very large-scale quasi-barotropic components of the motion. Much of the validity is lost when trying to describe the dynamics of the smaller-scale baroclinic developments which occur sporadically as extratropical cyclogenesis. This is probably the major reason why geostrophic and balanced baroclinic models on the average give no better wind forecasts at 500 mb than do barotropic models. The effects of released latent heat are on still a smaller scale, and the inertial-gravitational modes of atmospheric motion become even more important, if not essential. The divergent components appear to be of consequence not only in dynamical interactions but also for a proper accounting of the moisture budget.

There therefore seems to be no question that further progress will depend on our ability to construct an adequate dynamical framework. Until quite recently, attempts to integrate numerically the primitive equations had not succeeded. However some progress has now been achieved in devising a stable system for numerically integrating the primitive equations for baroclinic flow [*Smagorinsky*, 1958; *Hinkelmann*, 1959] as well as for barotropic flow [*Phillips*, 1959]. This experience is now being applied to the construction of a near-hemispheric, four-level model allowing moist adiabatic processes. This model will include the baroclinic as well as barotropic orographic effects and also a simple accounting of boundary layer processes.

It is apparent that the much smaller scale convective motions pose a special problem. It would, of course, be impractical to consider describing them by explicit dynamics. Ideally desirable is an adequate statistical-dynamical theory of moist convection which can define the classes of unstable ambient states and account for the systematic nonlinear interaction between the convective motions and the larger scale motions resolvable by explicit dynamics. Some work in this direction has been done by *Malkus* and *Witt* [1958] for dry convection. Moist convection, on the other hand, seems to be inherently different mechanistically and considerably more difficult to cope with. However, there is promise that numerical model experiments will yield further insight into the moist convective process, and work is now being undertaken in this direction.

Some gross properties of the macrophysics of condensation and precipitation—Until now the limitations of the hydrodynamic contexts did not warrant refinements in the assumptions regarding the physics of condensation. However, contiguous studies have indicated the way toward a somewhat more adequate linkage of the large-scale hydrodynamics and the condensation process. In

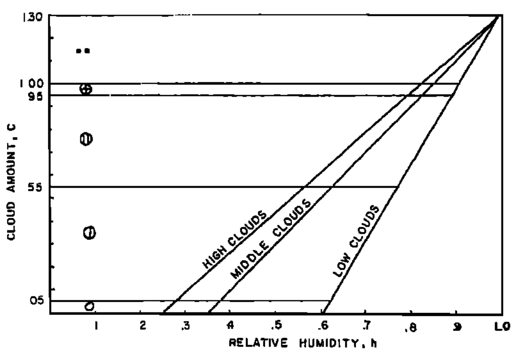

FIG. 1—Empirically determined relation of mean relative humidity h in the layers 1000–800 mb, 800–550 mb, and 550–300 mb with cloud amount c classed as low, middle, and high, respectively

particular, it would be desirable to allow for the non-precipitating cloud stage, since until now only a distinction between clear sky and precipitation has been attempted.

It is generally known that cloudiness and even precipitation are found to occur at space-averaged relative humidities considerably less than 100%. This cannot be dismissed as a purely instrumental aberration. Humidity as measured by the instrument and averaged from the sounding, represents the mean of a frequency distribution of smaller-scale humidity variations with considerable standard deviation. This must mean that for values of the average humidity considerably less than 100%, some condensation may be occurring due to saturation at the high end of the distribution. One would then expect that the amount or density of condensation (that is cloudiness) will increase with increasing mean humidity. Furthermore, one may view precipitation as resulting from sustained and very dense condensation, sufficient to create large enough particles, say for example by coalescence or the ice crystal process, to overcome the upward vertical currents.

Indeed one does find empirically that non-convective cloud amount, classed as low, middle, and high, is highly correlated with the average relative humidity in the respective layers. Precipitation, if interpreted as corresponding to a cloud amount somewhat greater than 1.0, also fits such a correlation. In fact, the simple linear relation

$$c = \beta h - \alpha \geq 0 \tag{1}$$

for each layer yields an excellent fit. Here c is the cloud amount, h is the relative humidity in per cent, and α and β are empirical coefficients. The fact that the instantaneous value of c does not appear to depend on the instantaneous vertical velocity is not surprising. One would expect non-precipitating condensation to depend only on the accumulated history of the vertical motion, which after all is reflected in the humidity.

For the purpose of establishing the coefficients α and β, it was assumed that the mean relative humidity in the 1000–800 mb layer corresponded to the span of low cloudiness, 800–550 mb to middle cloudiness, and 550–300 mb to high cloudiness. A graph of the linear relations is shown in Figure 1. (The writer is grateful to S. Hellerman for his assistance in determining this relation from careful analysis of a substantial volume of synoptic data.) It is of interest that all three levels tend to converge to $c = 1.3$ for $h = 1.0$.

It is well known that in the lowest 100 mb next to the Earth's surface humidities close to 100% are necessary before condensation is observed. This of course is due to the relatively intense mixing in the boundary layer. When surface winds are light, condensation in the form of fog may occur with lower humidities, but still considerably higher than in the 'free' atmosphere. It is of interest that non-industrial haze, which may be regarded as low-density fog, also occurs at high humidity. Under normal surface wind conditions, the intensely mixed layer is capped by an inversion through which the turbulence subsides almost discontinuously, and it is above the inversion that some condensation may occur at humidities as low as 60%.

The empirical relations found in no way are intended to reflect this discontinuous turbulence structure in the 1000–800 mb layer, but rather to give a measure of the integrated effect of turbulence in the entire layer. To account adequately for the finer grain structure of turbulence would require far greater vertical resolution and more refined techniques than have been employed here. One could guess as to what Figure 1 would look like if 'low clouds' were stratified according to the mean relative humidity (a) between 800 mb and cloud base, and (b) between cloud base and 1000 mb. For (a) the standard deviation of relative humidity would be larger than the mean in the 1000–800 mb layer due to weaker mixing so that condensation could occur at lower mean relative humidities. Curve (a) would then intercept the $c = 0$ axis at $h \approx 0.45$. Since the most intense mixing would be confined to the layer next to the ground, the frequency distribution of relative humidity would be very peaked. The curve (b) would intercept $c = 0$ at $h \approx 0.85$ or 0.90. Of course in this boundary layer c no longer corresponds to cloud amount but rather to the visibility which in the absence of industrial pollutants is fairly good measure of liquid water content in clouds as well as in fog [*Houghton* and *Radford*, 1938]. The fact that the visibility decreases with increasing relative humidity for humidities over 70% [see, for example, *Neiburger* and *Wurtele*, 1949] tends to support the above supposition.

An effective means for demonstrating the 'goodness of fit' of Figure 1 is to deduce cloud amount from synoptic radiosonde data only and to compare with 'actual' cloud observations, recognizing that the upper-level clouds when obscured from below must be estimated. All possible data including airways reports were employed. The comparisons are shown in Figures 2 and 3, for two cases, late spring and late fall. Included also are the geopotential fields at the 1000-, 700-, and 500-mb levels. The comparisons in the vicinity of the mountains must be ignored since the low-level humidities are fictitious and the observed cloud layers correspond to lower pressures than do sea-level observations.

The two cases shown in Figures 2 and 3 are from wholly independent data. However, the empirical linear relations of Figure 1 have been found extremely useful as an analysis aid in regions of sparse radiosonde data such as over the oceans. Moreover, even over continental U. S. the radiosonde network is often inadequate to fix the phase of smaller-scale distributions of humidity such as are associated with frontal zones.

The surprisingly good relation between liquid water content and water vapor suggests a means for incorporating the cloud stage in the water budget, and in fact will lead to a measure of the efficiency of moist adiabatic processes in large-scale condensation. Since cloud cover is a relative two-dimensional measure of liquid water, if we assume the vertical extent of large-scale (non-convective) clouds to be proportional to a linear measure of the horizontal dimension, then the volumetric measure of liquid water W is proportional to $c^{3/2}$. Defining W_1 as the minimum liquid water content necessary for precipitation, which according to Fig. 1 corresponds to $c = c_1 = 1$, then

$$W = W_1 c^{3/2} \tag{2}$$

We denote by the subscript 2 the condition when $h = 1$, so that $c_2 = 1.3$. We may now write the continuity equations for mixing ratio r, mass of liquid (cloud) water per unit mass of air W, and mass of precipitating water per unit mass of air W_P, assuming that water vapor may change by expansional condensation or compressional evaporation, but that precipitating water does not evaporate

$$\frac{dr}{dt} = \delta \frac{\gamma_m}{p} r_s\omega \begin{cases} \delta = 0 \text{ for } c = 0 \\ 0 < \delta \leq 1 \text{ for } 0 < c \leq c_2, \end{cases} \tag{3}$$

$$\frac{dW}{dt} = (\delta^* - \delta) \frac{\gamma_m}{p} r_s\omega$$
$$\cdot \begin{cases} \delta^* = 0 \text{ for } c \leq c_1 \text{ or } \omega \geq 0 \\ 0 \leq \delta^* \leq 1 \text{ for } c_1 \leq c \leq c_2 \text{ and } \omega < 0 \end{cases} \tag{4}$$

$$\frac{dW_P}{dt} = -\delta^* \frac{\gamma_m}{p} r_s\omega \tag{5}$$

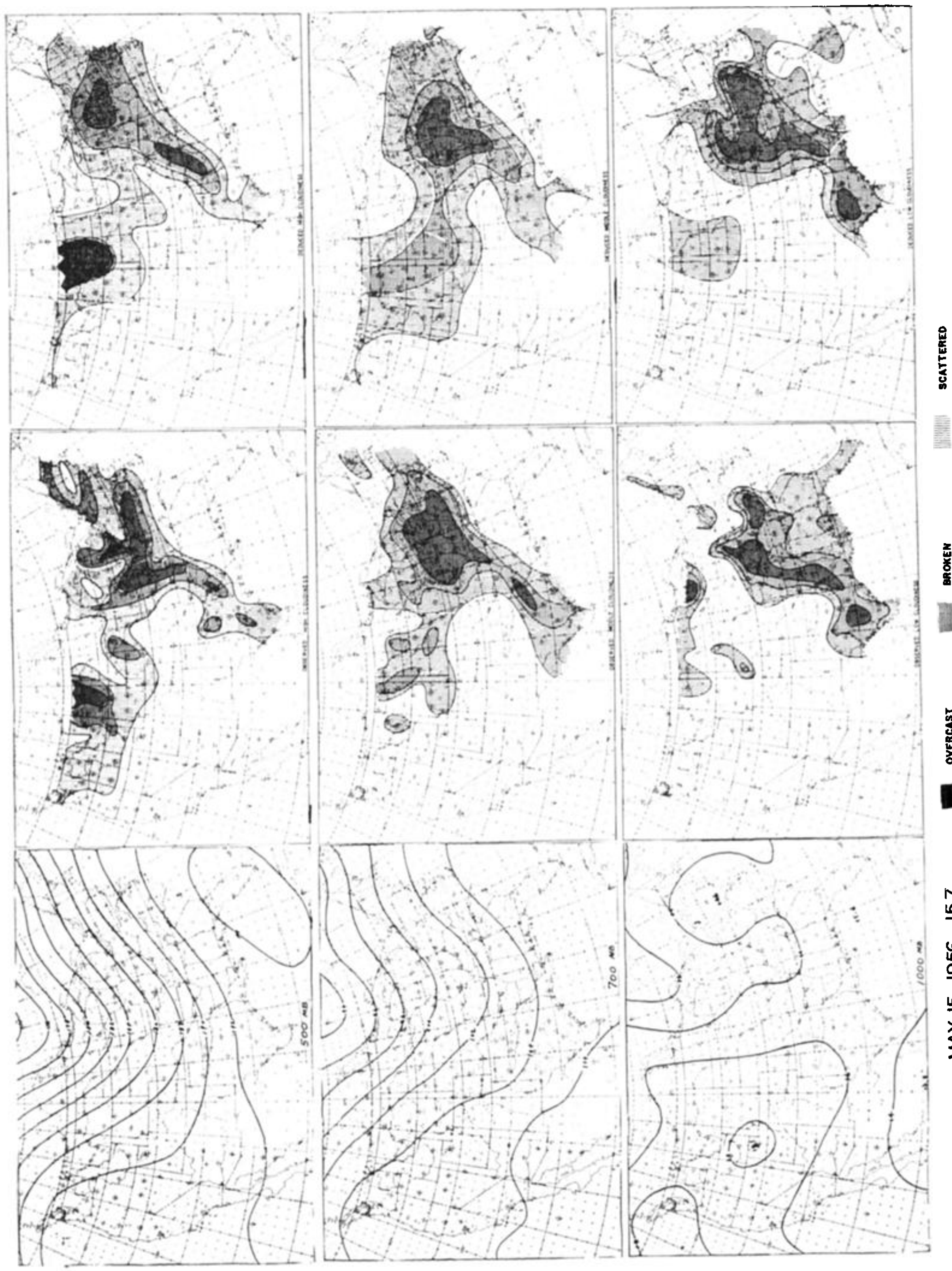

FIG. 2—From right to left: cloudiness deduced from humidity soundings and the empirical relations in Figure 1, observed cloudiness, observed geopotential; late spring

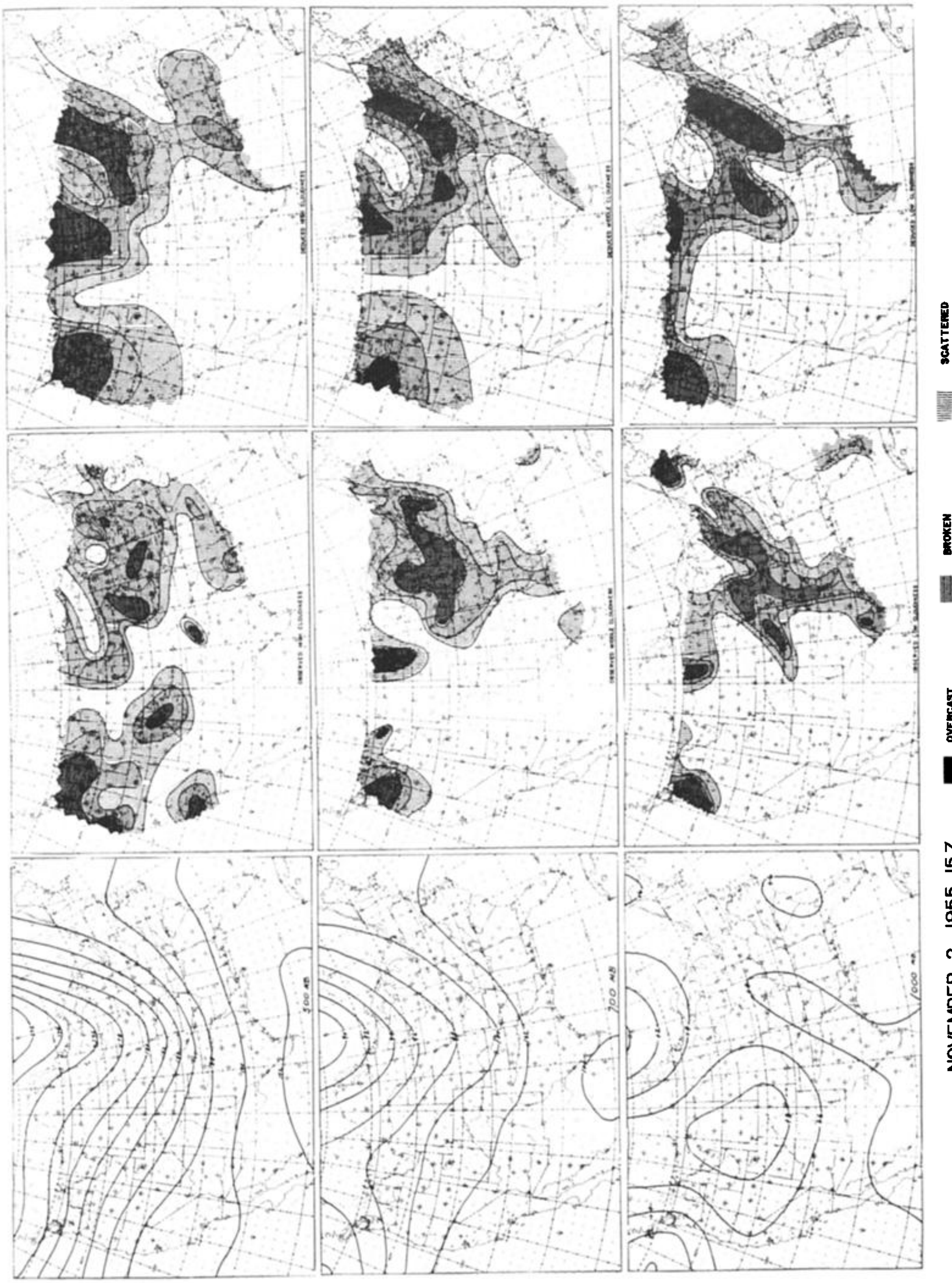

Fig. 3—From right to left: cloudiness deduced from humidity soundings and the empirical relations in Figure 1, observed cloudiness, observed geopotential; late fall

and the precipitation rate is

$$P = \int (1/g\rho_W) \frac{dW_P}{dt}\, dp \tag{6}$$

The potential temperature θ change due to such condensation or evaporation is given by

$$\frac{d \ln \theta}{dt} = \delta \frac{\Gamma}{p} \omega \tag{7}$$

The notation is as follows: p is the pressure, g is the acceleration of gravity, ρ_W is the density of water, $\omega \equiv dp/dt$, r_s is the saturation mixing ratio, δ is the fraction of mass undergoing moist adiabatic processes, and δ^* is the fraction of condensing water being precipitated. Also

$$\gamma_m(T, p) \equiv p \left(\frac{d \ln r_s}{dp}\right)_{\theta_E = \mathrm{const}} = \frac{\kappa\gamma + \alpha - 1}{\alpha\gamma - \alpha + 1} > 0. \tag{8}$$

$$\Gamma(T, p) \equiv p \left(\frac{d \ln \theta}{dp}\right)_{\theta_E = \mathrm{const}} = -\alpha \left(\frac{\kappa\alpha - \kappa - 1}{\alpha\gamma - \alpha + 1}\right) < 0 \tag{9}$$

where

$$\alpha(T, p) \equiv \frac{Lr_s}{c_pT} \tag{10}$$

$$\gamma(T) \equiv \frac{L}{R^*T} \tag{11}$$

and T is the absolute temperature, θ_E the equivalent potential temperature, L is the latent heat of condensation or sublimation, $(1 - \kappa) = c_v/c_p$ is the ratio of the specific heat of air at constant volume to that at constant pressure, R^* is the gas constant for water vapor $\approx 4.62 \times 10^6$ cm^2 sec^{-2} deg.$^{-1}$

Unlike δ^* which is zero for $\omega \geq 0$, δ does not depend on ω since downward motion of a cloud parcel must result in dynamic evaporation so that $dW/dt < 0$ and $dr/dt > 0$. We are not free to specify arbitrarily δ since (1) and (2) must be satisfied simultaneously by (3) and (4). Ignoring variations in α, β, and W_1, then (1) and (2) require that

$$\frac{dW}{dt} = \frac{3}{2} \beta W_1 \sqrt{c} \frac{dh}{dt} \tag{12}$$

Since by definition

$$r = hr_s \tag{13}$$

then

$$\frac{dh}{dt} = \frac{1}{r_s}\left(\frac{dr}{dt} - h \frac{dr_s}{dt}\right) \tag{14}$$

The first term, the change of h caused by a change in water vapor, is given by (3); the second term also depends on the fraction of mass undergoing moist adiabatic changes δ, but of course does not vanish for purely dry adiabatic processes, since it changes with temperature and may be written as

$$\frac{dr_s}{dt} = r_s\omega[\delta\gamma_m + (1 - \delta)\gamma_d], \tag{15}$$

where

$$\gamma_d(T) \equiv p \left(\frac{d \ln r}{dp}\right)_{\theta = \mathrm{const}} = \kappa\gamma - 1 > 0, \tag{16}$$

and it may easily be verified that

$$\Gamma = \frac{\gamma_m - \gamma_d}{\gamma} = \kappa \frac{\gamma_m - \gamma_d}{1 + \gamma_d} \tag{17}$$

Hence

$$\frac{dh}{dt} = \left[(1 - h)\delta \frac{\gamma_m}{p} - (1 - \delta)h \frac{\gamma_d}{p}\right] \omega \tag{18}$$

Inserting (4) and (18) into (12) yields

$$\delta = \frac{\delta^* + \chi h \sqrt{c}\, \gamma_d/\gamma_m}{1 + \chi \sqrt{c}\,[(1 - h) + h\gamma_d/\gamma_m]} \tag{19}$$

where

$$\chi \equiv 1.5\beta W_1/r_s \tag{20}$$

For $c \leq c_1$, we have that $\delta^* = 0$ so (19) and (1) uniquely define δ as a function of c or h. Also, for $c_1 \leq c \leq c_2$ and $\omega \geq 0$, we have that $\delta^* = 0$, again uniquely defining δ. On the other hand, when $\omega < 0$, we have $\delta_1^* = 0$ as before, and since all condensing water vapor must be precipitating when $c = c_2$ then by (4) $\delta_2 = \delta_2^* = 1$. Assuming δ^* to vary linearly in this range then

$$\delta^* = \frac{c - c_1}{c_2 - c_1} = \frac{c - 1}{0.3} \geq 0 \text{ for } c_1 \leq c \leq c_2,\ \omega < 0 \tag{21}$$

We furthermore see that a maximum liquid water is attained for $c = c_2$, which by (2) is

$$W_2 = W_1 c_2^{3/2} \tag{22}$$

Hence the maximum liquid water content is 50%

larger than the threshold liquid water content below which precipitation cannot occur. There is some empirical evidence [*aufm Kampe* and *Weickmann,* 1957; *Mason,* 1957, p. 231] that such a maximum exists, its value depending on the type of cloud. This is reasonable since the precipitation drop size and hence W_1 should depend on the characteristic magnitude of the vertical velocities working against gravity. For stratiform clouds, with a characteristic vertical velocity of 5 cm sec^{-1}, $\rho W_2 \approx 0.5$ gm m^{-3} (ρ is the air density); while for Cumulus clouds, with vertical velocities of the order of 50 m sec^{-1}, $\rho W_2 \approx 5$ gm m^{-3}. *Komabayasi* [1957] suggests that ρW_2 varies as the $1/3$ power of the vertical velocity. We have then for stratiform clouds that $\rho W_1 \approx 0.3$ gm m^{-3}.

One would expect ρW_2 for non-convective clouds to be a maximum in mid-troposphere ($\approx$550 mb) where ω is a maximum in the large scale; this is consistent with the findings of *aufm Kampe* and *Weickmann* [1957], who report much lower liquid water contents at the Cirrus level. However, for the purpose of estimating the variation of δ with h in different cloud layers we use an average value of $\rho W_1 = 0.3$ gm m^{-3}, and furthermore assume the temperature to vary as in the standard atmosphere. The corresponding values of the parameters occurring in (1), (19), (20), and (21) are given in Table 1. Figure 4 shows δ as a function of h and c for each of the three tropospheric layers for which α and β have been determined empirically. Figure 4 indicates that for ascending motion the maximum rate of increase of liquid water, which is proportional to $\delta - \delta^*$, is attained just as precipitation begins. As the mean relative humidity increases beyond this point, $\delta - \delta^*$ decreases until $dW/dt = 0$ at $h = 1$. Under continued upward motion the condensing water is directly precipitated. On the other hand for downward motion of an existing cloud the rate of conversion of liquid water to water vapor, which is proportional to δ, has a maximum at $h = 1$ and decreases monotonically to $c = 0$.

The net effect is a process analogous to that resulting from entrainment in Cumulus development, but on a smaller scale. The fact that mean relative humidities of 100% are not often observed even from precipitating clouds must mean a significant dilution of the moist adiabatic process during precipitation. Hence even larger upward vertical velocities than calculated on the assumption of no dilution ($\delta = \delta^* = 1$) are necessary to explain the amounts of large-scale precipitation observed.

TABLE 1—*Values of parameters used in constructing Figure 4*

Layer	α	β	ρ	r_s	γ_d	γ_m
mb			10^{-3} gm cm^{-3}	gm kg^{-1}		
550–300 (high)	0.433	1.733	0.6	1.1	6.2	5.3
800–550 (middle)	0.70	2.0	0.9	3.7	5.0	2.9
1000–800 (low)	2.0	3.33	1.1	7.9	4.6	2.4

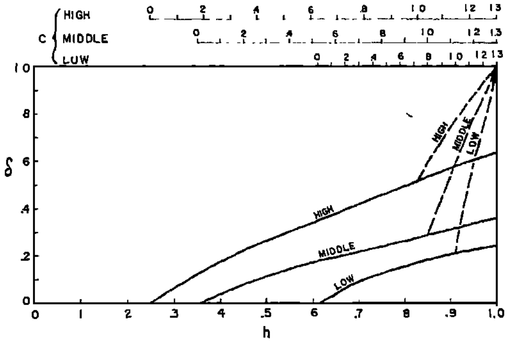

FIG. 4—The percentage of mass undergoing moist adiabatic processes δ as a function of relative humidity h for low, middle, and high clouds; the corresponding cloud amount c is given along the upper abscissa; solid lines are for the non-precipitating stage, dashed lines are for the precipitating stage; for $0 < c \leq 1.0$, each curve is valid for $\omega \lessgtr 0$; for $1.0 \leq c \leq 1.3$ the solid line is valid for $\omega \geq 0$ and the dashed line for $\omega < 0$

REFERENCES

AUBERT, E. J., On the release of latent heat as a factor in large scale atmospheric motions, *J. Met.*, **14**, 527–542, 1957.

AUFM KAMPE, H. J., AND H. K. WEICKMANN, Physics of clouds, *Met. Res. Rev.*, 1951–55, *Met. Monographs*, Amer. Met. Soc., **3**, 182–225, 1957.

HINKELMANN, K., Ein numerisches Experiment mit den primitiven Gleichungen, *C.-G. Rossby Memorial Volume*, Esselte A. B., Stockholm, 1959.

HOUGHTON, H. G., AND W. H. RADFORD, On the measurement of drop size and liquid water content in fogs and clouds, *Papers Phys. Oceanogr. Met., Mass. Inst. Tech. and Woods Hole Oceanog. Inst.*, *4*, 31 pp., 1938.

KOMABAYASI, M., Some aspects of rain formation in warm cloud (II), Liquid water content as a function of upward velocity, *J. Met. Soc. Japan*, **35**, 266–277, 1957.

MALKUS, J. S., AND G. WITT, The evolution of a convective element: a numerical calculation, *Woods Hole Oceanog. Inst. Cont. 967*, 1958.
MASON, B. J., *The Physics of Clouds*, Oxford Press, 1957.
MIYAKODA, K., Forecasting formula of precipitation and the problem of conveyance of water vapour, *J. Met. Soc. Japan*, 34, 212–225, 1956.
NEIBURGER, M., AND M. G. WURTELE, On the nature and size of particles in haze, fog, and stratus of the Los Angeles region, *Chemical Rev.*, 44, 321–335, 1949.
PHILLIPS, N. A., Numerical integration of the primitive equations on the hemisphere, *Mon. Wea. Rev.*, 87, no. 9, 1959.
SMAGORINSKY, J., AND G. O. COLLINS, On the numerical prediction of precipitation, *Mon. Wea. Rev.*, 83, 53–68, 1955.
SMAGORINSKY, J., On the inclusion of moist adiabatic processes in numerical prediction models, *Berichte des Deutschen Wetterdienstes 38*, pp. 82–90, Symposium über Numerische Wettervorhersage in Frankfurt a.M., 1956.
SMAGORINSKY, J., On the numerical integration of the primitive equations of motion for baroclinic flow in a closed region, *Mon. Wea. Rev.*, 86, 457–466, 1958.
SMAGORINSKY, J., AND COLLABORATORS, manuscript in preparation, 1959.
SMEBYE, S. J., Computation of precipitation from large-scale vertical motion, *J. Met.*, 15, 547–560, 1958.

Discussion

Mr. Jerome Namias—If the ultimate aim in all this is to predict in detail, at what point there may have to be a cut-off in this prediction scheme. It would have to make inferences about conditions responsible for run-away processes and various things down to some scale. That is, must we settle for a certain scale? I'd like to ask Dr. Smagorinsky if he believes there is no cut-off point and if he expects to go to the bitter end and attempt to predict weather on all scales by numerical process.

Dr. Joseph Smagorinsky—I would say that one can reasonably place a cut-off at the point where the statistical dynamics of the smaller scale motions are sufficiently stable and well understood. The ability to establish a threshold of turbulence permits the study of the explicit dynamics of the synoptic scale motion with adequate provision for the interaction with the scales of motion ultimately responsible for the dissipation of kinetic energy. Such a threshold of the horizontal scale appears to be of the order of 100 km. However, as I pointed out in my paper, the interaction of small scale convection with large scale motions is hardly understood.